Research Square

Preprints are preliminary reports that have not undergone peer review.
They should not be considered conclusive, used to inform clinical practice,
or referenced by the media as validated information.

Re-Visiting Monsoon Intra-Seasonal Variability from the perspective of Large-Scale Atmospheric Energetics

SOMENATH DUTTA

dutta.drsomenath@gmail.com

1. Former Scientist, India Meteorological Department, presently at Indian Institute of Tropical Meteorology and Savitribai Phule Pune University. https://orcid.org/0000-0003-0507-989X

Parthasarathi Mukhopadhyay

Ashoka University

Pallavi Prabhu

Savitribai Phule Pune University

Sanjay G Narkhedkar

Retired Scientist IITM

Research Article

Keywords: Monsoon Intra-seasonal variability, Energetics

Posted Date: October 30th, 2026

DOI: https://doi.org/10.21203/rs.3.rs-10775354/v1

License: This work is licensed under a Creative Commons Attribution 4.0 International License.
Read Full License

Re-Visiting Monsoon Intra-Seasonal Variability from the perspective of Large-Scale Atmospheric Energetics

Somenath Dutta[1], Parthasarathi Mukhopadhyay[2], Sanjay Narkhedkar[3] and Pallavi Prabhu[4]

1. Former Scientist, India Meteorological Department, presently at Indian Institute of Tropical Meteorology and Savitribai Phule Pune University.
2. Former Scientist, Indian Institute of Tropical Meteorology & Visiting faculty, IISER Bhubaneshwar and presently visiting professor, Ashoka University, Haryana
3. Former Scientist, Indian Institute of Tropical Meteorology
4. India Meteorological Department and Savitribai Phule Pune University.

Abstract

In this pilot study, an attempt has been made to revisit the problem of monsoon intra-seasonal variability (MISV) of the southwest monsoon from the perspective of large-scale atmospheric energetics. For that, daily values of two energy generation terms and four energy conversion terms for the period from 1 May to 30 September for the years 1979–2017, obtained from Dutta et al. (2019), have been used. These generation and conversion terms were computed using high-resolution (0.125° × 0.125°) daily re-analysed ERA-5 data of air temperature (T) and three components of wind () at standard isobaric levels, viz., 1000, 925,850, 700, 600, 500, 400, 300, 250, 200, 150, 100 hPa levels at 00 UTC over the domain 5°N–35°N, 65°E–95°E, during the above-mentioned period.

Results of this study suggest that the variability of atmospheric energetics of the Indian Summer Monsoon is fundamentally dominated by synoptic-scale variability (2–8 days) across all rainfall categories. At the same time, the occurrence, persistence, and intensity of lower-frequency oscillations (QBW, EQBW, MISO) vary systematically with monsoon strength. Energy generation terms are predominantly governed by synoptic disturbances, highlighting the primary role of monsoon depressions, low-pressure systems, and associated mesoscale weather systems in modulating the monsoon energy cycle. Energy conversion terms likewise exhibit statistically significant synoptic-scale variability in every ISMR category, suggesting that rapid baroclinic and barotropic energy conversions constitute the dominant mode of monsoon energetics irrespective of seasonal rainfall.

Overall, the results suggest that while synoptic disturbances dominate the monsoon energy cycle across all ISMR categories, the persistence and organization of quasi-biweekly and MISO-scale variability largely determine the efficiency and longevity of atmospheric energy generation and conversion in stronger monsoon years.

Keywords: Monsoon Intra-seasonal variability, Energetics

1. **Introduction:** The Asian summer monsoon is one of the most energetic components of the Earth's climate system. It is primarily driven by convective, radiative and sensible heat sources/sinks. Most of the annual rainfall in India occurs from June to September during the southwest monsoon. Two remarkable features of the summer monsoon are its regular occurrence from June to September and the irregular variation in the seasonal mean rainfall it brings to India from one year to another. There are many years with floods (strong monsoon) or droughts (weak monsoon), during which India as a whole receives excess or deficient seasonal rainfall, respectively. Even within a season, there is considerable variation in rainfall over India in both space and time, known as Monsoon Intra-Seasonal Variation (MISV).

Ramamurthy (1969), in an exhaustive analysis of daily rainfall over India, first documented vigorous intraseasonal oscillations of the Indian summer monsoon in the form of "active" and "break" rainfall spells within the season. Independently, Madden and Julian (1971), analyzing nearly a decade of daily rawinsonde data from Canton Island (3°S, 172°W), detected a significant 41–53-day periodicity in the co-spectrum of the 850- and 150-mb zonal wind components — the first report of an eastward-propagating oscillation in the tropical atmosphere, now known as the Madden-Julian Oscillation (MJO). A shorter, 10–20-day fluctuation was subsequently identified in various monsoon parameters by Krishnamurti and Bhalme (1976) and in cloudiness data by Yasunari (1979).

The Tropical Convergence Zone (TCZ) over the Indian monsoon region represents the ascending branch of the regional Hadley circulation, and its fluctuations — first identified in Indian station data by Keshavamurthy (1973) and Dakshina Murthy and Keshavamurthy (1976) — were later shown to be coherent with fluctuations of the regional Hadley circulation (Krishnamurti & Subramaniam, 1982; Murakami et al., 1984; Mehta & Krishnamurti, 1988; Hartmann & Michelsen, 1989) and with northward-propagating Monsoon Intraseasonal Oscillations, or MISOs (Sikka & Gadgil, 1980). The active and break spells of the monsoon are thus associated with fluctuations of the TCZ (Yasunari 1979, 1980, 1981; Sikka & Gadgil, 1980). More broadly, the intraseasonal oscillations (ISOs) of the Indian summer monsoon form a broadband spectrum with periods between 10 and 90 days, but with two preferred bands — 10–20 days and 30–60 days (Krishnamurti & Bhalme, 1976; Krishnamurti & Ardanuy, 1980; Yasunari, 1980). This 10–90-day fluctuation between wet and dry spells is a general feature of the tropics, referred to as tropical intraseasonal variability (Lau & Waliser, 2012).

The most distinctive character of MISV over India is the occurrence of active periods, with heavy rainfall over central India, alternating with break periods, in which rainfall over central India is weak or absent while northern and south-eastern India receive above-normal rainfall; each phase typically persists for a few days. Given its influence on agriculture and public health, MISV carries substantial socio-economic significance for the country.

MISV during the summer monsoon season spans timescales from a few days to over a month and is shaped by (at least) two distinct modes of variability. The dominant, large-scale mode is the slowly evolving intraseasonal oscillation (ISO), marked during the northern summer by an apparent northward movement of convection originating over the central equatorial Indian Ocean. A second, synoptic-scale mode consists of westward-propagating convective disturbances with timescales of 5–10 days; westward-propagating wave activity of this kind intensifies during the active phase of the large-scale ISO. The high-frequency convective disturbances that develop over the Bay of Bengal and peninsular India are generally attributed to instability favoured by strong easterly vertical wind shear acting in conjunction with equatorial heating.

The active-break cycle, and its link to fluctuations in the strength of the continental and oceanic TCZ, has repeatedly been tied to the 30–60-day intraseasonal oscillation (Yasunari, 1979; Sikka & Gadgil, 1980; Gadgil & Asha, 1992). Several studies (Yasunari, 1979; Lau & Chan, 1986; Singh & Kripalani, 1985; Annamalai & Slingo, 2001) have additionally reported eastward propagation of convection associated with the northward-propagating TCZ on this same timescale, implying that the MJO (Madden & Julian, 1972) also modulates the active-break cycle of monsoon rainfall; Hartmann and Michelsen (1989) confirmed a corresponding spectral peak in 1901–70 daily rainfall data. Across these studies, the intraseasonal variation of the Indian monsoon is consistently dominated by the 10–20-day and 30–60-day bands, with the 10–20-day mode contributing less than the 30–60-day mode to the total intraseasonal variability, as judged by their relative contributions to convective heating.

Lawrence (1999) showed that the boreal summer ISO exhibits two somewhat different evolutions. Both are characterized by convection coupled to a Kelvin-Rossby wave packet that moves steadily eastward. However, they differ in how convection over the central Indian Ocean develops ahead of the mature wave packet: the “south-north” mode begins with a largely stationary development of equatorial convection, whereas the “east-west” mode shows eastward propagation of convection

anomalies from the outset. South-North events tend to occur early in the monsoon season, when equatorial Indian Ocean SSTs are at their peak, while East-West events typically occur later, once the SSTs have cooled somewhat.

The 30–60-day mode is most active during the monsoon onset phase and shows less coherent propagation through the remainder of the summer (Annamalai & Slingo, 2001) while the 10–20-day mode is linked to westward-propagating disturbances originating in the western Pacific (Krishnamurti & Ardanuy, 1980); these disturbances also play a role in re-establishing the active monsoon phase after a break, through the genesis of new disturbances within the monsoon zone. Annamalai and Slingo (2001) further argue that the 10–20-day mode is more regional in character, with its influence confined largely to the local Hadley circulation. Neither mode is strictly periodic; both instead appear as two dominant bands in the spectra of rainfall, outgoing longwave radiation (OLR) and circulation data, together explaining only about 10–25% of the daily variance in the NCEP-NCAR reanalysis circulation data (Goswami et al., 1998), with the 30–60-day mode contributing more than the 10–20-day mode (Annamalai & Slingo, 2001) and with zonal propagation proving more robust than meridional propagation (Goswami et al., 1998). Notably, the character of this intraseasonal variability does not differ appreciably between major drought and major flood years (Krishnamurthy & Shukla, 2000; Annamalai & Slingo, 2001).

Separating summertime ISOs by their zonal propagation characteristics over the Indian Ocean and western Pacific, Lawrence and Webster (2002) showed that eastward propagation of convection along the equator is a fundamental feature of most summertime ISOs — 42 of the 54 ISOs exhibiting northward movement, or 78%, also showed eastward propagation — and that this eastward propagation is directly related to the northward movement of convection associated with the active-break cycle of precipitation across India. Building on this, Sperber and Annamalai (2008) identified five characteristic features of the boreal summer ISO (BSISO): eastward propagation over the eastern equatorial Indian Ocean; extension of the equatorial convective mode across the Maritime Continent; northward propagation near India; north-westward propagation over the west Pacific; and the characteristic tilted rainband.

A fundamental and defining characteristic of the summer ISO is the northward movement of convection, beginning over the central equatorial Indian Ocean and terminating near the foothills of the Himalaya in northern India (Lawrence & Webster, 2002). This northward movement has been documented extensively by Murakami 1976; Yasunari 1979, 1980, 1981; Sikka and Gadgil 1980; Krishnamurti and Subrahmanyam 1982; Singh

and Kripalani 1985; Lau and Chan 1986; Wang and Rui 1990). The similarity between the ISO timescale and the cycling time from active to break to active conditions over India led Yasunari (1979), and subsequently Julian and Madden (1981) and Lau and Chan (1986), to propose that the northward movement of convection is linked to the eastward-propagating cloud bands along the equator (see Madden and Julian 1994 for a review). Wang and Rui (1990), however, identified a summertime mode that behaves as an independent northward-moving event with no accompanying eastward movement of convection along the equator, and which may therefore be unrelated to the MJO.

More recent process-based studies have examined the physical mechanisms underlying this propagation. Abhik et al. (2015), using eleven years (1998–2008) of TRMM data together with MERRA reanalyses, examined the role of cloud hydrometeors and associated dynamical parameters in the northward propagation of the BSISO, finding that during strong BSISO events, hydrometeors such as cloud liquid water, precipitable ice and cloud ice show a steady northward progression from the equatorial Indian Ocean to about 25°N. Using a Lagrangian dynamic recycling model applied to ECMWF-ERA-Interim reanalysis data, Pathak et al. (2017) traced the moisture transported to the Indian landmass from oceanic and terrestrial sources at intraseasonal timescales. They found that oceanic moisture sources are associated with the north-south pattern of intraseasonal rainfall variation. In contrast, the Ganga basin — the principal terrestrial source — is associated with the east-west pattern extending from the Core Monsoon Zone to eastern India.

Recent studies have further refined the understanding of boreal summer intraseasonal oscillation (BSISO) / monsoon intraseasonal oscillation (MISO). Kottapalli and Vinayachandran (2025) showed that equatorial convection is the primary source of BSISO amplitude and northward propagation in both present and future climates; under SSP370 projections, BSISO rainfall is enhanced by about 63 % over the Bay of Bengal and 42 % over the Arabian Sea, while the proportion of northward-propagating events remains largely unchanged. They also noted that the background moisture gradient remains largely unchanged in the future, so the proportion of northward-propagating BSISO events remains nearly the same even as rainfall intensity increases. Konda et al. (2026) reported a strong twofold increase in Indian summer monsoon intra-seasonal variability under high-emission scenarios, accompanied by faster phase speeds of northward-propagating ISOs and a reduction in the northwest–southeast tilt of the precipitation band. Their analysis further suggests that the increased magnitude of precipitation anomalies associated with the northward-propagating ISOs may intensify

active monsoon spells and raise the frequency of extreme rainfall events over India. Lin et al. (2025) showed that northward-propagating convective phases of the ISO are sustained by horizontal moisture advection, and moist-static-energy tendencies are particularly triggers of monsoon onset over the Arabian Sea and India, with ENSO modulating the background meridional asymmetry. Waje et al. (2025) further showed that the Quasi-Biennial Oscillation independently modulates the persistence and spatial extent of active and break spells of the Indian summer monsoon. During the easterly phase of the QBO, the active spells become more persistent and spatially extended, while the break spells become shorter and weaker; the opposite occurs during the westerly QBO phase.

Li et al. (2022) examined the kinetic energy budget of the cyclonic vortex associated with MISO. They found that the pronounced intraseasonal kinetic energy is mainly attributable to barotropic energy conversion from the background circulation. They further found that energy conversion from the mean flow is stronger ahead of the vortex (due to interactions between intraseasonal easterlies and downdrafts). In contrast, after the vortex, the conversion is mainly due to interactions between intraseasonal westerlies and updrafts. Lu et al. (2025) diagnosed the energy budget of the dominant interannual modes of the South Asian summer monsoon and highlighted the contrasting roles of barotropic and baroclinic energy conversions.

Energetics is a very useful tool for explaining various atmospheric processes/phenomena dynamically. From the foregoing discussions, there are hardly any studies addressing the MISV problem from an energetic aspect. The objective of this study is to revisit the MISV problem from the perspective of large-scale atmospheric energetics.

From the foregoing discussion, it appears that most studies on Indian Summer monsoon intra-seasonal variability use primary data, such as daily rainfall, OLR, horizontal wind, and cloud-pixel data.

It is worth noting that ISMR is the final output of various dynamical and thermodynamical processes, such as the reverse Hadley circulation, the Walker circulation, monsoon-midlatitude flow interactions, diabatic heating, convective instability, etc. It is therefore envisaged that, alongside the well-documented ISO of ISMR, the intraseasonal variability of the individual metrics representing these driving processes will be examined to arrive at a more complete dynamical interpretation of the ISO of ISMR.

Accordingly, in this study an attempt has been made to revisit Monsoon Intra-seasonal variability/oscillation from the perspective of large-scale atmospheric energetics,

performing standard power spectrum analysis and wavelet analysis on the time series of daily composite anomaly (1 May-30 Sept during 1979-2017) of six large scale atmospheric energetics parameters, viz., Generations of Zonal Available Potential Energy & Eddy Available Potential Energy, Conversions of Zonal Available Potential Energy to Zonal Kinetic Energy, Eddy Available Potential Energy to Eddy Kinetic Energy, Zonal Available Potential Energy to Eddy Available Potential Energy and Zonal Kinetic Energy to Eddy Kinetic Energy, for deficient, below-normal, normal, above normal and excess all India Summer monsoon rainfall (AISMR) categories. These daily composite values of the above-mentioned parameters have been obtained from the study of Dutta et al. (2019).

In Section 2, details of the data used and their source have been discussed; in Section 3, brief details of the methodology used have been discussed; Section 4 has been dedicated to a comprehensive discussion of the results obtained; in Section 5, we have summarised the story addressed in this study, and finally, in Section 6, pointwise conclusions have been given.

2. Data: For carrying out this study, daily values of two energy generation terms four energy conversion terms, & during the period from 1 May to 30 September for the years 1979–2017, obtained from the study of Dutta et al. (2019), have been used. In addition, daily, monthly, and seasonal rainfall data for these years during the summer monsoon season from the India Meteorological Department, India, have been used.

3. Methodology: Dutta et al., (2019) computed above mentioned two energy generation terms and four energy conversion terms, using high resolution (0.125° × 0.125°) daily re-analysed ERA-5 data of air temperature (T) and three components of wind () at standard isobaric levels, viz., 1000, 925,850, 700, 600, 500, 400, 300, 250, 200, 150, 100hPa levels at 00 UTC over the domain 5°N–35°N, 65°E–95°E, during the period from 1 May to 30 September for the years 1979–2017. The detailed formulation of these energetic parameters is given in Table 1. From the daily values of the above-mentioned energetics parameters and their mean (based on the period from 1979 to 2017), the daily anomalies of each of them for all 153 days from 1 May to 30 September have been computed. Afterwards, a daily composite of anomalies has been constructed for the deficient, below normal, normal, above normal, and excess categories of All India Summer Monsoon Rainfall (AISMR), following IMD criteria (as given in Table 2). Composite anomaly time series of values of two energy generation terms & and four energy conversion terms have then been subjected to power spectrum analysis and

wavelet analysis, using the Morlet wavelet function. C. Torrence and G. Compo provided wavelet software, which is available at URL: http://atoc.colorado.edu/research/wavelets/.

4. Results and analysis: In this section, results on performing power spectrum analysis and wavelet analysis on the composite series of two generations and four conversion terms, as mentioned above, for deficient, below normal, normal, above normal and excess ISMR cases are discussed. In the following sub-section, the analysis of results for two generation terms and four conversion terms is discussed. For each of them, results from power spectrum analysis are first discussed, followed by those from wavelet analysis.

4.1. Generation of ZAPE $[G(A_Z)]$:

4.1.1. **Interpretation**: Generation of zonal available potential energy (A_Z), denoted by $G(A_Z) = \frac{R_d}{C_p}\oint \frac{[\theta]^*[\dot{Q}]^*}{p\left(-\frac{\partial\bar{\theta}}{\partial p}\right)}dm$. For its interpretation, we have $[\theta]^* = \frac{\partial[\theta]}{\partial y}\delta y \; and \; [\dot{Q}]^* = \frac{\partial[\dot{Q}]}{\partial y}\delta y$. Thus $G(A_Z)$represents the process of integrated combined effect of meridional gradient of diabatic heating and that of temperature. With a given N-S temperature gradient, an enhanced diabatic heating (and/or cooling) over warmer (and/or colder) latitudes results in an enhanced generation of A_Z.

4.1.2. **Power spectrum analysis**: Power spectrum analysis (PSA) of $G(A_Z)$ for all composite cases are shown in fig 1(a-e).

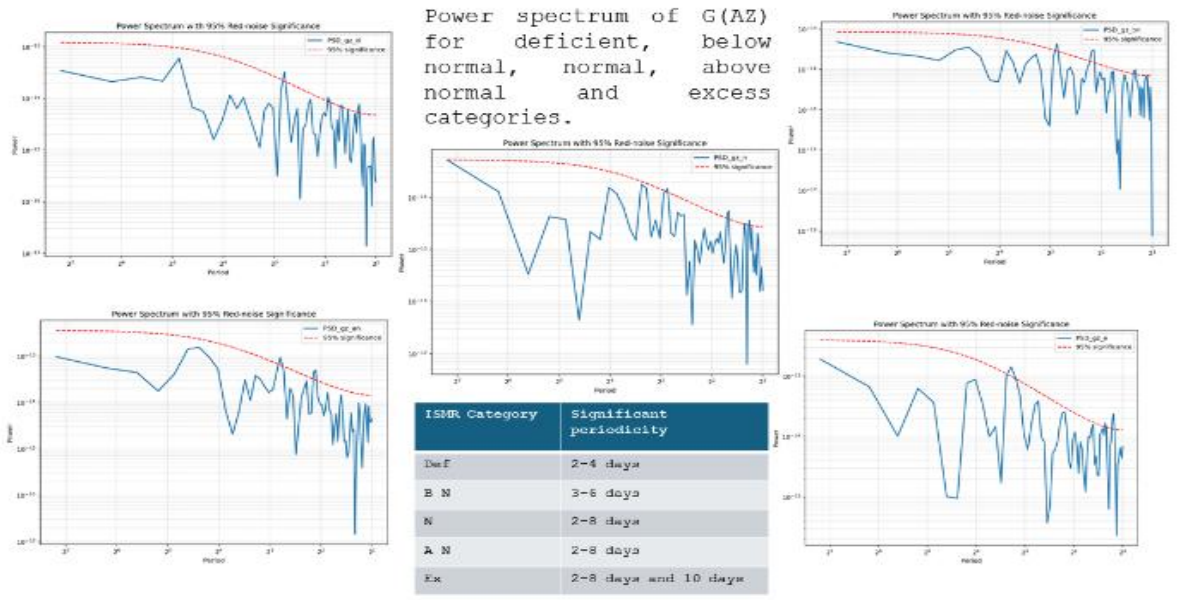


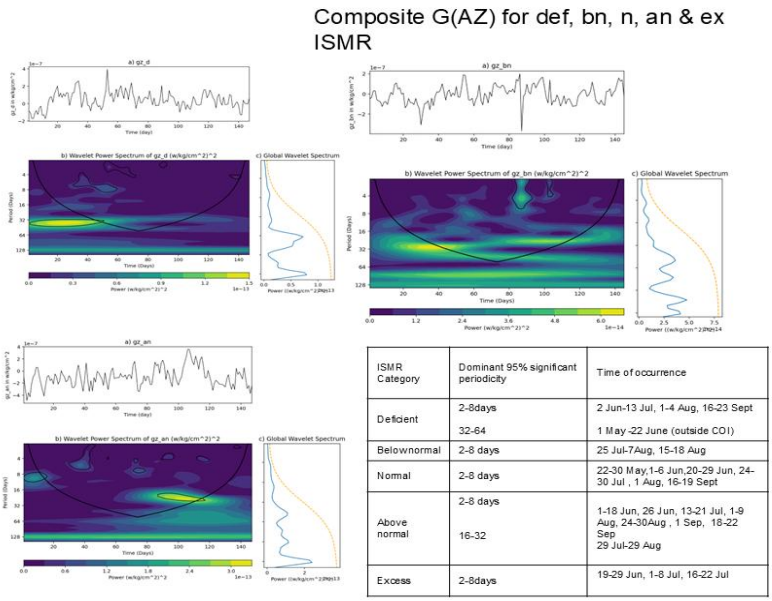
Fig.1 : PSA of $G(A_Z)$for (a) deficient (b)below normal (c) normal (d) above normal (e) excess categories

From the figure, it is seen that the dominant statistically significant periodicities in $G(A_Z)$ occur in the **2–8-day band**, for all ISMR categories. However, a significant periodicity near 10 days is also observed in the excess ISMR category. But in any case, there is no significant peak in any category of ISMR in the 10–20–day (QBWO) and 30–60–day (MISO) bands.

The presence of statistically significant 2–8-day periodicities in all ISMR categories implies that the generation of zonal available potential energy is fundamentally a synoptic-scale process and the dominant coherent oscillations in $G(A_Z)$ are associated with the life cycle of monsoon weather systems rather than seasonal active-break oscillations.

However, the appearance of an additional significant ~10-day peak only during excess ISMR suggests that the quasi-biweekly oscillation becomes dynamically important only when the monsoon circulation is sufficiently strong. In such cases, enhanced latent heating organises the generation of ZAPE on quasi-biweekly time scales. Thus, for the excess ISMR category, $G(A_Z)$ exhibits both synoptic scale and quasi-biweekly variability.

4.1.3. **Wavelet analysis**: Wavelet analysis of $G(A_Z)$ for all composite cases is shown in the adjoining fig 2(a-e).



ISMR Category	Dominant 95% significant periodicity	Time of occurrence
Deficient	2-8days	2 Jun-13 Jul, 1-4 Aug, 16-23 Sept
	32-64	1 May -22 June (outside COI)
Belownormal	2-8 days	25 Jul-7Aug, 15-18 Aug
Normal	2-8 days	22-30 May,1-6 Jun,20-29 Jun, 24-30 Jul , 1 Aug, 16-19 Sept
Above normal	2-8 days	1-18 Jun, 26 Jun, 13-21 Jul, 1-9 Aug, 24-30Aug , 1 Sep, 18-22 Sep
	16-32	29 Jul-29 Aug
Excess	2-8days	19-29 Jun, 1-8 Jul, 16-22 Jul

Fig.2 : Wavelet analysis of $G(A_Z)$for (a) deficient (b)below normal (c) normal (d) above normal (e) excess categories

From the figure, it is seen that for all ISMR categories, statistically significant variability of this energetics parameter is concentrated in the **2–8-day synoptic band** scattered across the season, emphasising the dominant role of synoptic disturbances in modulating the meridional covariance between diabatic heating and temperature gradients. Besides, the emergence of an excess QBM in the above-normal category in August suggests occasional quasi-biweekly organisation of the heating field.

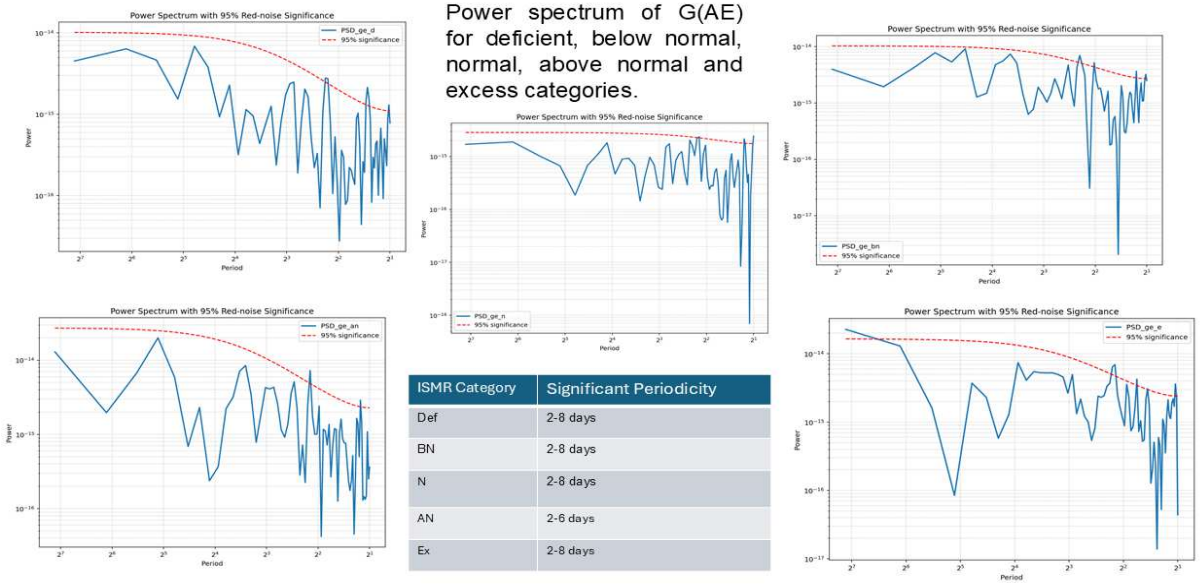
4.2. **Generation of EAPE $[G(A_E)]$:**

4.2.1. **Interpretation**: Generation of eddy available potential energy (A_E) is mathematically expressed as

$G(A_E) = \frac{R_d}{C_p}\oint \frac{\theta'\dot{Q}'}{p\left(-\frac{\partial\bar{\theta}}{\partial p}\right)}dm$. Here, $\dot{Q}' = \frac{\partial \dot{Q}}{\partial x}\delta x \; and \; \theta' = \frac{\partial \theta}{\partial x}\delta x$. Thus, $G(A_E)$ represents the process of integrated combined effect of zonal gradient of diabatic heating and that of temperature. With a given E-W temperature gradient, an enhanced diabatic heating (and/or cooling) over warmer (and/or colder) longitudes results in an enhanced generation of A_E.

4.2.2. **Power spectrum analysis**: Power spectrum analysis of $G(A_E)$, along with significant periodicities, for all composite cases is shown in the adjoining figure 3(a-e).

It is seen that for all IMSR categories, composite anomaly of $G(A_E)$ has significant periodicity at 2-8 days only. Thus, **Generation of EAPE is a synoptic-scale process during the Indian summer monsoon**, with significant variability concentrated in the **2–**



ISMR Category	Significant Periodicity
Def	2-8 days
BN	2-8 days
N	2-8 days
AN	2-6 days
Ex	2-8 days

Fig.3 : PSA of $G(A_E)$for (a) deficient (b)below normal (c) normal (d) above normal, (e) excess categories

8-day band across all ISMR categories. From the absence of persistent low-frequency power it may be suggested that **large-scale intraseasonal oscillations modulate the occurrence of synoptic systems indirectly**, whereas the direct generation of EAPE remains fundamentally a synoptic-scale process.

4.2.3. **Wavelet analysis:** Wavelet analysis of $G(A_E)$ is given in the adjoining figure 4(a-e).

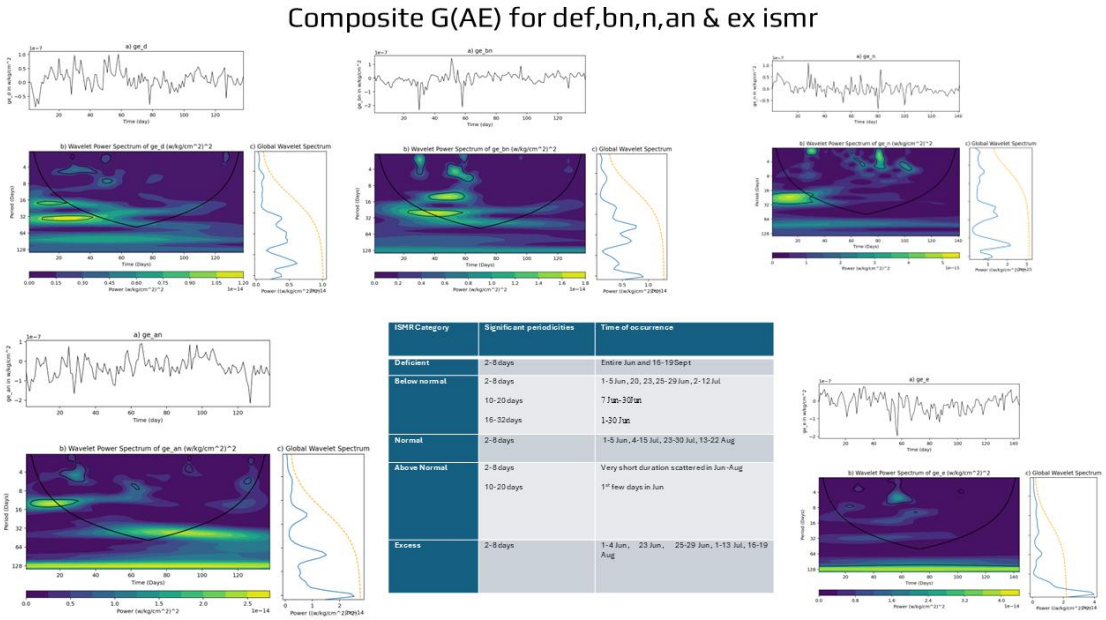


Fig.4 : Wavelet analysis of $G(A_E)$for (a) deficient (b)below normal (c) normal (d) above normal (e) excess categories

Results of the wavelet analysis are seen to be echoing that of power spectrum analysis. From the figure it is seen that the statistically significant periodicities of composite daily anomaly of $G(A_E)$ are primarily confined to the synoptic (2–8 days) in all AISMR category. In deficient category it is in June and 3rd week of September, below normal categories during 1st and last week of June in the 1st two weeks in July, in normal category it is during 1st week of June, 2nd week of July, last week of July and 3rd week of August, in above normal category it occurred in scattered way from June to August and in excess category in early June, late June, early July & mid-August. Besides, there is emergence of quasi biweekly mode (10-20 days) in below & above normal categories and an Excess QBM (16-32 days) in below normal categories, both in June. Thus, in above-normal/excess years showed stronger, more robust synoptic-scale G(EAPE) generation than deficient years.

4.3. **Conversion of A_Z to A_E[$C(A_Z, A_E)$]:**

4.3.1. **Interpretation**: Conversion of A_Z to A_E, denoted by

$C(A_Z, A_E) = -\int_{100}^{P_s}\left[\frac{1}{\sigma}\overline{v'T'}\frac{\partial \overline{T^*}}{a\,\partial\emptyset} + \frac{1}{\sigma}\overline{\omega'T'}\frac{\partial \overline{T^*}}{\partial p}\right]dp$. This term represents the strength of the combined effect of two processes, viz., eddy meridional flux of temperature in presence

meridional gradient of temperature $\left(\frac{\partial T^*}{a\,\partial \emptyset}\right)$ and vertical flux of temperature under different static stability conditions.

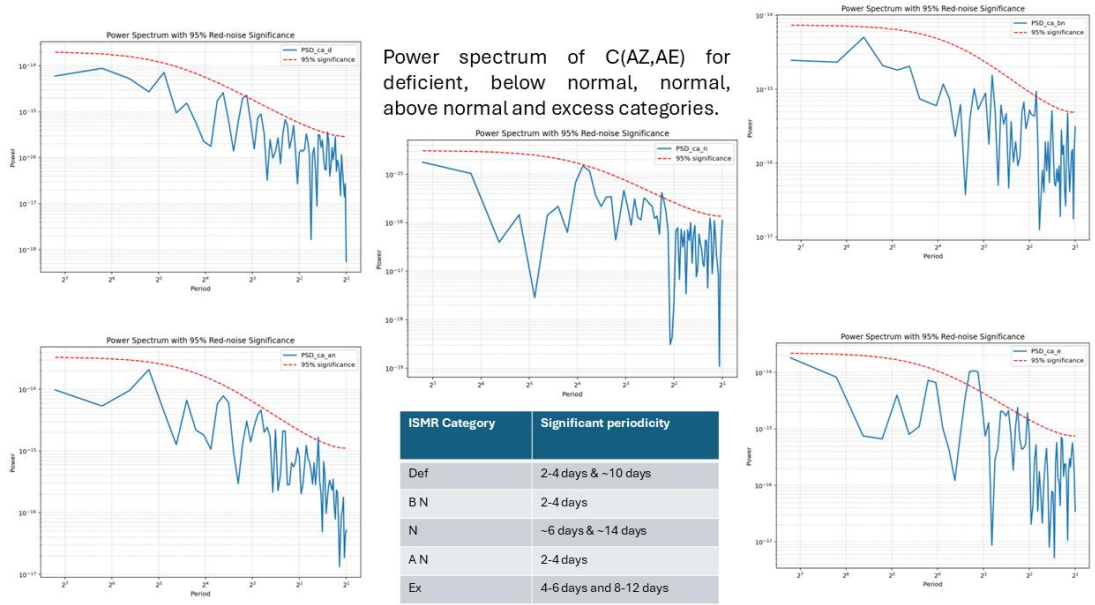
If the zonal mean temperature is warmer towards north, then the meridional gradient of temperature, $\frac{\partial T^*}{a\,\partial \varphi} > 0$. Then eddy southerly/northerly transport of colder/warmer air $(\overline{v'T'} < 0)$ converts ZAPE to EAPE in a stably stratified condition.

In the region of study, during ISMS, $\frac{\partial T^*}{a\,\partial \varphi} > 0$. Hence in the presence of any synoptic scale weather system (LOW/WML/D/DD) over this region, there is southerly (northerly) cold (warm) air transport to the eastern (western) flank and thus converting ZAPE to EAPE.

In case of a mid-latitude westerly belt, where $\frac{\partial T^*}{a\,\partial \emptyset} < 0$, the northerly cold air advection ($\overline{v'T'} >$), $associated$ with southward protruding baroclinic waves embedded in the mid-latitude westerly mean flow, results in the reduction in meridional temperature gradient over ISM region, leading to a reduction in ZAPE at the cost of generation of EAPE, thus leading to conversion of ZAPE to EAPE.

For the second term, when there is a local convective instability over any latitudinal belt in the region of study, then $-\frac{\partial T^*}{\partial z} > \frac{g}{C_p} \Rightarrow \frac{\partial T^*}{\partial p} > \frac{\alpha}{C_p} > 0$. Then rising motion $(\omega < 0)$ of warmer $(T' > 0)$ air associated with the convection results in the conversion of ZAPE to EAPE.

4.3.2. **Power spectrum analysis**: Plots of power spectrum analysis of daily composite anomaly of this energetics parameter for all ISMR categories are shown in the adjoining figure 5(a-e).



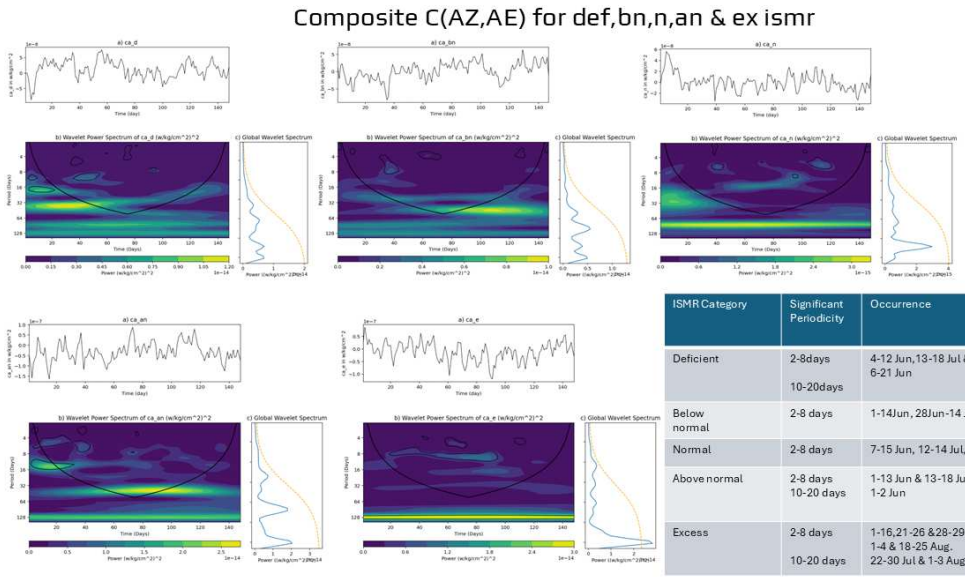
ISMR Category	Significant periodicity
Def	2-4 days & ~10 days
B N	2-4 days
N	~6 days & ~14 days
A N	2-4 days
Ex	4-6 days and 8-12 days

Fig.5 : PSA of $\boldsymbol{C(A_Z, A_E)}$ for (a) deficient (b)below normal (c) normal (d) above normal (e) excess categories

From the above PSA and the attached table, one can find four types of significant periodicities exhibited by daily composite anomaly series of $C(A_Z, A_E)$, viz., high frequency (2-8 days) variation exhibited in all categories of ISMR and Quasi-Bi Weekly Variations (10-20 days) in Deficient (Def), normal & Excess (Ex) categories.

High frequency variation in Deficient & Below Normal categories indicates that even in suppressed monsoon years (Def/BN), rapid synoptic-scale waves are still extracting energy baroclinically from the mean flow. Quasi Bi-Weekly variation in excess category indicates prolonged constructive interference (between monsoon and mid latitude flow) that continuously extracts ZAPE to fuel active monsoon spells and that in deficient categories indicates a highly episodic, short-lived energy extractions, spaced widely apart, keeping the overall monsoon in a net deficit. Quasi Bi-Weekly variation in normal category may be interpreted as the mean meridional temperature gradient over India accumulates ZAPE over a week, collapses as baroclinic instability triggers widespread rainfall via eddies, converting ZAPE to EAPE and then takes roughly another week to rebuild.

i. **Wavelet analysis**: Plots of the Wavelet analysis, performed on the time series of composite anomaly of $C(A_Z, A_E)$ for different ISMR categories, are shown in Figure 6(a-e).



ISMR Category	Significant Periodicity	Occurrence
Deficient	2-8days 10-20days	4-12 Jun,13-18 Jul & 2-6 Aug 6-21 Jun
Below normal	2-8 days	1-14Jun, 28Jun-14 Jul,6-12 Sept
Normal	2-8 days	7-15 Jun, 12-14 Jul, 12-30 Aug, 25-29 Sept
Above normal	2-8 days 10-20 days	1-13 Jun & 13-18 Jul. 1-2 Jun
Excess	2-8 days 10-20 days	1-16,21-26 &28-29 Jun, 1-14 & 26-30 Jul and 1-4 & 18-25 Aug. 22-30 Jul & 1-3 Aug

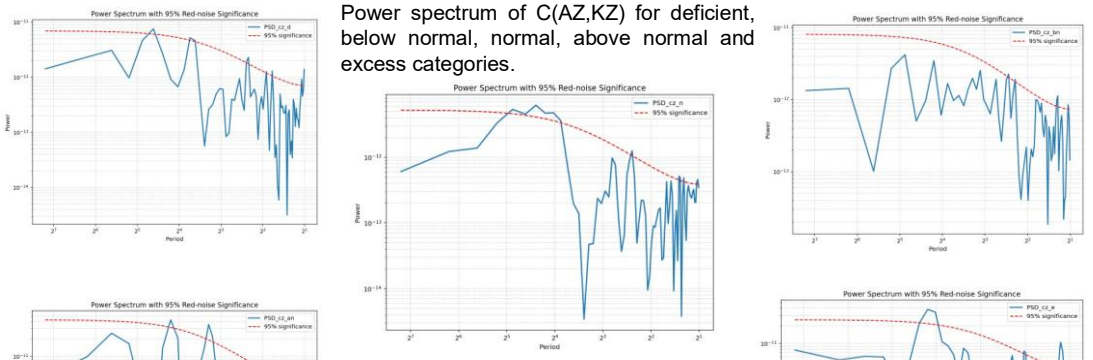
Fig.6: Wavelet analysis of $\boldsymbol{C(A_Z, A_E)}$ for (a) deficient (b)below normal (c) normal (d) above normal (e) excess categories

The figure shows presence of two modes, viz., high frequency synoptic scale (2-8 days) and a slow ISO scale QBM (10-20 days) mode occurring at different times in the season. In deficient category 10–20 day signal is active during 6–21 June and bursting of 2–8 day mode in early June, mid-July, early August; in below Normal category only 2–8 day activity, spread across June, late June–mid July, and early-mid September; in normal ISMR category both bands (2-8 days & 10-20 days), spans from June through late September; in above normal category 2–8 day dominant through June–mid July, with a brief 10–20 day window (1–2 June) and in excess ISMR category both bands very active, with extended and overlapping windows from June through August (the most persistent/energetic signal of all categories).

Thus, Synoptic-scale (2–8 day) energy conversion between zonal and eddy available potential energy is a persistent feature of C(AZ, AE) across all five rainfall categories. A robust intraseasonal / quasi-biweekly (10–20 day) signal is additionally present in the Deficient, Normal and Excess categories, but is absent (or not statistically significant) in the Below Normal and Above Normal categories. Intraseasonal band is most persistent and energetic in the Excess category and most episodic in the Deficient category, while the Normal category shows the broadest temporal extent of significant activity across the season.

4.4.1. **Interpretation**: Conversion of A_Z to K_Z, $C(A_Z, K_Z)$ is mathematically expressed as $C(A_Z, K_Z) = -\frac{1}{g}\int_{100}^{P_s} \frac{R}{p}\overline{\omega^* T^*} dp$. From this expression it is seen that there is a conversion from A_Z to K_Z, provided the vertically integrated effect of the covariance in the integral is negative. This is possible if there is stronger rising motion over warmer latitudinal belt and/or stronger sinking motion over colder latitudinal belt. Thus, this term is a metric of the strength of thermally direct circulation in meridional-vertical (y-z/y-p) plane.

4.4.2. **Power spectrum analysis**: Power spectrum analysis (PSA), performed on the series of daily composite anomaly of $C(A_Z, K_Z)$ for different ISMR categories. PSA plots are shown in the adjoining figure 7(a-e).



Power spectrum of C(AZ,KZ) for deficient, below normal, normal, above normal and excess categories.

ISMR Category	Significant period
Deficient	2-8 days, 10-20days & 16-32 days
Below Normal	2-8 days
Normal	2-8 days & 16-32 days
Above Normal	2-8 days, 10-20days & 16-32 days
Excess	2-8 days & 16-32 days

Fig.7 : PSA of $\boldsymbol{C(A_Z, K_Z)}$ for (a) deficient (b)below normal (c) normal (d) above normal (e) excess categories

From this figure and the attached table, it is seen that high-frequency periodicity (2-8 days) in $C(A_Z, K_Z)$ is present across all ISMR categories, indicating that basic synoptic-scale kinetic energy generation continues to occur even during poor monsoon seasons.

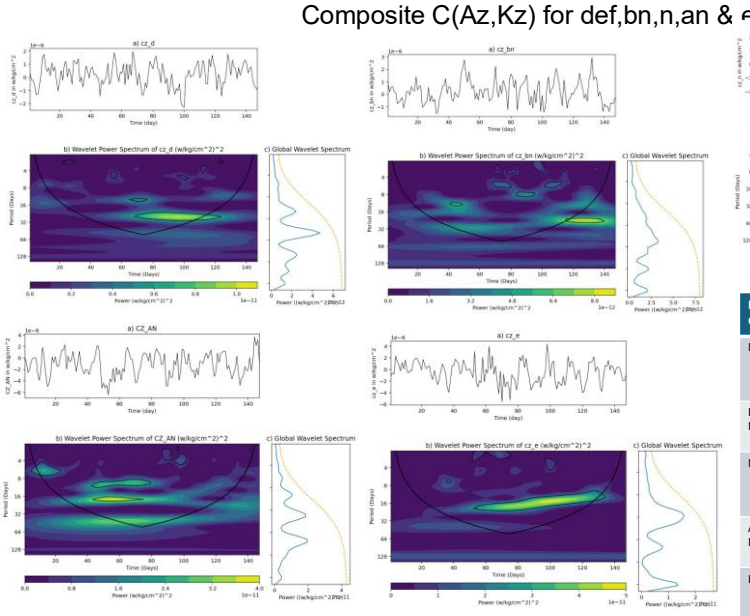
From the table, it can also be seen that the quasi-biweekly oscillation (10-20 days) appears explicitly in **Deficient** and **Above Normal** conditions. In the **Above Normal** scenario, it represents a highly efficient, rhythmically repeating surge where the meridional thermal contrast (ZAPE) regularly accelerates the mean monsoon circulation (ZKE), whereas in the Deficient scenario, the energetic cycle becomes strictly trapped or restricted to this timescale. The overturning divergent circulation in the y-z plane lacks the power to sustain longer-period loops, forcing the background energetics to oscillate sharply between brief structural stabilisation and collapse.

Significant low frequency intra-seasonal oscillation near 16-32 days is seen in normal, above normal, excess categories and deficient categories. Existence of this mode in normal, above normal & excess categories **indicates** that atmosphere has been able to sustain these deep, multi-week planetary-scale baroclinic conversion cycles, whereas, in **Deficient / Below Normal years**, this planetary-scale conversion loop breaks down entirely. The large-scale thermal engine fails to convert ZAPE into ZKE at this low frequency.

The appearance of this **quasi-biweekly mode** in deficient and above-normal categories suggests intermittent quasi-biweekly modulation superimposed on the dominant ~20-day oscillation.

Thus, in **surplus (N, AN, Ex) categories** the conversion of ZAPE to ZKE works seamlessly across all scales—from quick synoptic bursts up to planetary-scale 28-day planetary loops, whereas, in deficit **(Def, BN)** categories ZAPE-to-ZKE conversion cannot be sustained at the 16–28 day scale, i.e., the mean monsoon flow is not efficient for low-frequency energy generation and must rely purely on short-lived synoptic and biweekly pulses.

4.4.3. Wavelet analysis: Results of wavelet analysis, performed on the daily composite anomaly of conversion of ZAPE to ZKE for different ISMR categories, are shown in fig 8(a-e). From the figure and the attached table, it is seen that for all categories of ISMR, the composite anomaly possesses significant oscillation in the synoptic scale (2-8 days),quasi-biweekly (10-20 days) & excess quasi-biweekly (16-32 days) range, with one MISO range (30-60 days) in the normal ISMR category.



ISMR Category	Significant periodicities	Occurrence
Deficient	2-8 days 10-20days 16-32 days	23-26 Jun, 7-13 Aug, 22-25 Aug &4-5 Sept. 6 July-17July Entire Aug
Below-Normal	2-8 days 10-20 days 16-32 days	9 Jul-25 Aug 11-18 Jun 27 -30 Aug
Normal	2-8 Days 10-20days 16-32days 30-60 days	19 -29 Jun, 1-3 Jul, 6-16 Aug Jun-29 to Aug-05 1 Jul-4 Sept 11 Jul-12 Aug
Above Normal	2-8 days 10-20days 16-32 days	28 Jul-12 Aug & 22-24 Sept 13June – 15 July 14June – 15 July
Excess	2-8 days 10-20days 16-32 days	6-8 Jun, 22 Jun-16 Jul & 8-14 Aug 10 Jul- 15 Sept 23 Jun-20 Aug

Fig.8 : Wavelet analysis of $\boldsymbol{C(A_Z, K_Z)}$ for (a) deficient (b)below normal (c) normal (d) above normal (e) excess categories

In the deficit category (Below normal and Deficient) this oscillation occurred for a short duration (7-11 days) in June and July, whereas, in surplus category (Above normal & excess) it occurred for a longer periods, viz., from mid-June to mid-July and mid-June to mid-September.

Thus in the surplus category of ISMR, the mean monsoon circulation in the y-z plane is repeatedly and reliably strengthened on a ~2-week periodicity throughout the season, whereas in the deficit category same is for a brief period, Deficit category is also characterised by re-energisation of the mean monsoon circulation in the y-z plane on a ~3-4 week periodicity at the later part of the season. Besides, as expected in all categories the synoptic-scale (~2–8 day) mode is present in a scattered way during different times in the season. This scale physically interprets synoptic scale weather systems, like monsoon lows/depressions, mid-latitude westerly interacting with monsoon circulation, etc. During the genesis, intensification or decaying of such systems, locally distortion of latitudinal thermal gradient takes place locally, which in turn strengthens or

weakens/disrupts the mean monsoon circulation in the y-z plane on a short timescale, which is demonstrated as a short-lived pulse of C(ZAPE,ZKE) power at 2–8 days, superimposed on the slower QBWO envelope.

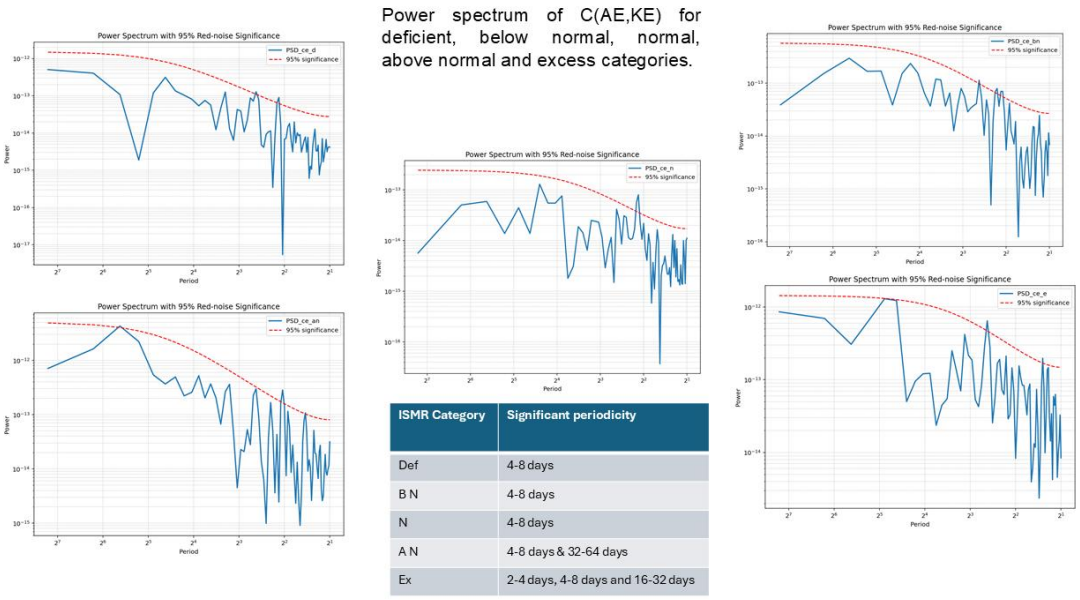
4.5. **Conversion of Eddy available potential energy to eddy kinetic energy** [$\boldsymbol{C(A_E, K_E)}$].

4.5.1. **Interpretation**: Conversion of EAPE to EKE is given by, $C(A_E, K_E) = -\frac{1}{g}\int_{100}^{P_s} \frac{R}{p}\overline{\omega' T'} dp$. The covariance in the integrand is the covariance of two departures from zonal mean, viz., the departure of 'ω' from its zonal mean ω^* and that of 'T' from its zonal mean T^*. Thus there is a conversion of EAPE to EKE, if the vertically integrated effect of this covariance is negative, which is possible if there is stronger rising motion over warmer longitude and/or stronger sinking motion over colder longitude around a given latitudinal belt. So, this term may be thought of as a measure of the strength of thermally direct circulation in zonal-vertical (x-z/x-p) plane. This term is also known as baroclinic eddy kinetic energy conversion.

4.5.2. **Power spectrum analysis**: Plots of Power spectrum analysis (PSA), performed on the time series of daily composite anomaly of $C(A_E, K_E)$ for different ISMR categories for May-September months, are shown in figure 9(a-e).

From the PSA analysis, performed on the time series of daily composite anomaly of this energetics parameters for different ISMR categories, it is revealed that the modulation of the **conversion of EAPE to EKE is primarily dominated by high frequency synoptic-scale (2–8 day) mode across all ISMR categories**, implying the importance of monsoon lows, depressions and mesoscale convective systems in maintaining eddy kinetic energy.

476



ISMR Category	Significant periodicity
Def	4-8 days
B N	4-8 days
N	4-8 days
A N	4-8 days & 32-64 days
Ex	2-4 days, 4-8 days and 16-32 days

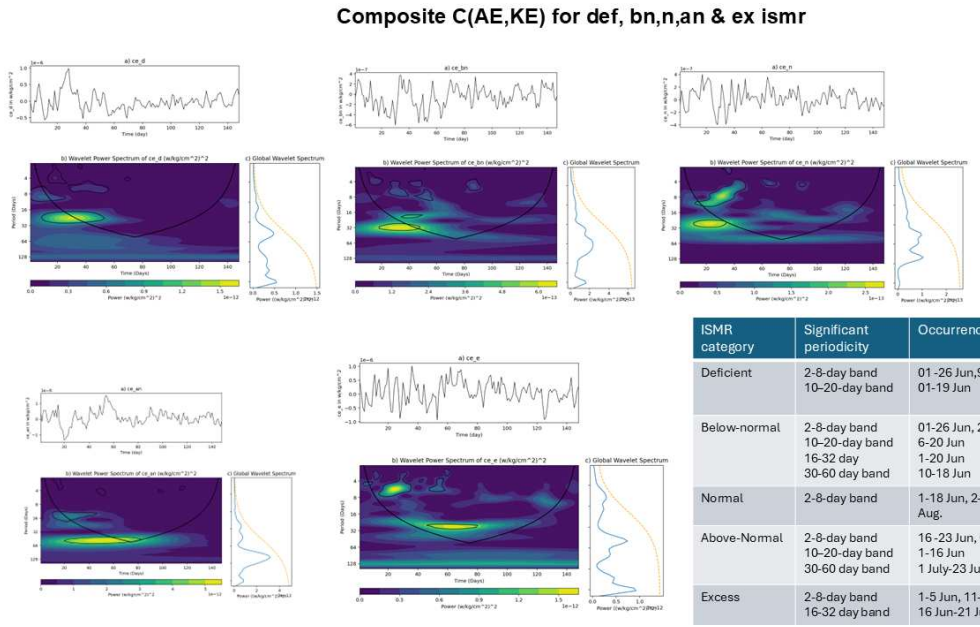
Fig.9 : PSA of $\boldsymbol{C(A_E, K_E)}$ for (a) deficient (b)below normal (c) normal (d) above normal (e) excess categories

477

478 For surplus categories (AN & Ex), excess quasi biweekly (16-32 days) and MISO (32-
479 64) modes are also present. The appearance of longer-period oscillations only in **above-**
480 **normal and excess monsoons** indicates that stronger rainfall seasons possess a more
481 organized multiscale eddy energy cascade.

482 Presence of 2-8 days band in *every* ISMR category, suggests that baroclinic eddy kinetic
483 energy conversion via these transient systems is a persistent, background feature of the
484 monsoon. It doesn't switch off even in deficient years, though its amplitude and shape do
485 change slightly. Emergence of 32-64 days band in above-normal years implies that when
486 rainfall is enhanced, energy conversion is being modulated not just by fast synoptic
487 eddies but also by the slower large-scale ISO. Co-existence of three significant bands,
488 viz., 2–4 days, 4–8 days, and 16–32 days in the excess ISMR category suggests that
489 excess-rainfall years are characterized by multi-scale energy conversion process, rather
490 than being driven by a single dominant timescale.

4.5.3. **Wavelet analysis**: Wavelet analysis has been performed on the time series of daily composite anomaly of $C(A_E, K_E)$ for different ISMR categories for May-September months. Plots of the same are shown in figure 10 (a-e).



ISMR category	Significant periodicity	Occurrence
Deficient	2-8-day band 10–20-day band	01 -26 Jun,9-12Jul 01-19 Jun
Below-normal	2-8-day band 10–20-day band 16-32 day 30-60 day band	01-26 Jun, 23 -30 Jul, 01 – 03Aug. 6-20 Jun 1-20 Jun 10-18 Jun
Normal	2-8-day band	1-18 Jun, 2-11 Jul, 28-30 Jul, 1-3 Aug.
Above-Normal	2-8-day band 10–20-day band 30-60 day band	16 -23 Jun, 08 -11 Aug, 25-28 Aug 1-16 Jun 1 July-23 July
Excess	2-8-day band 16-32 day band	1-5 Jun, 11-13 Jun, 18 Jun-2 Jul 16 Jun-21 Jul

Fig.10 : Wavelet analysis of $\boldsymbol{C(A_E, K_E)}$ for (a) deficient (b)below normal (c) normal (d) above normal (e) excess categories

From the plots and the attached table, it can be seen that for the deficient ISMR category, **the time series broadly consists two significant modes, viz., a** single, well-defined quasi-biweekly mode (10–20-day band), with significant power concentrated broadly in the first half of June and high frequency Synoptic-scale (2–8 day), with comparatively week power intermittently in June and first half of July. This suggests that during deficient monsoon seasons, eddy energy conversion is governed primarily by the quasi-biweekly oscillation, without substantial reinforcement from higher-frequency synoptic disturbances.

In the below normal category, the time series is seen to be dominated by the co-existence of multi-scale variability, viz., synoptic scale (2-8 days) during most of the time in June, from last week of July through the end of first week of August, Quasi-biweekly (10-20 days) and Excess Quasi-biweekly (16-32 days) in the first three weeks in June and finally Monsoon intra-seasonal oscillation during 2nd and 3rd week of June. Thus, the synoptic disturbances interact with larger-scale intraseasonal variability during monsoon onset and larger scale signals decay rapidly after June, indicating that the multiscale organization is not maintained through the season.

From the figure it is seen that in normal ISMR category the time series is dominated mainly by synoptic scale (2-8 days) variations, indicating that baroclinic conversion is maintained primarily through recurring synoptic systems rather than strong low-frequency modulation.

In the above normal ISMR category, this conversion is dominated by high frequency synoptic scale (2-8 days) in the 2nd half of June & 2nd and 4th week of August, Quasi biweekly oscillation (10-20 days) in first half of June and MISO (30-60 days) during the

first three weeks of July. Long-duration signature of this mode suggests that above-normal rainfall seasons are associated with a sustained, large-scale intensification of the Walker circulation in mid monsoon, supporting prolonged enhanced-ascent conditions over the Indian sector.

In the excess ISMR category this energy conversion is dominated by high frequency synoptic scale disturbances, occurring scattered in June and Extended QBW oscillation from mid-June to Mid-August. Thus, in this category the Walker circulation is reinforced twice, first transiently by active synoptic disturbances, then more sustainedly by a later intraseasonal oscillation.

Thus, the synoptic-scale (2–8 day) variability is the fundamental mode of $C(A_E, K_E)$ across all ISMR categories, indicating the importance of synoptic scale weather systems in ISM, like monsoon depressions, lows and synoptic disturbances in converting eddy available potential energy into eddy kinetic energy. The persistent presence of intraseasonal oscillations only distinguishes the behaviour of this energy conversion mechanism, i.e., the Walker circulation among different ISMR categories. In the Deficient years conversion is short-lived during early-season, whereas in the above-normal and excess monsoon years the sustained 16–32-day and/or 30–60-day variability helps to maintain efficient baroclinic energy conversion over extended periods. This multiscale interaction is consistent with prolonged active monsoon spells and enhanced seasonal rainfall.

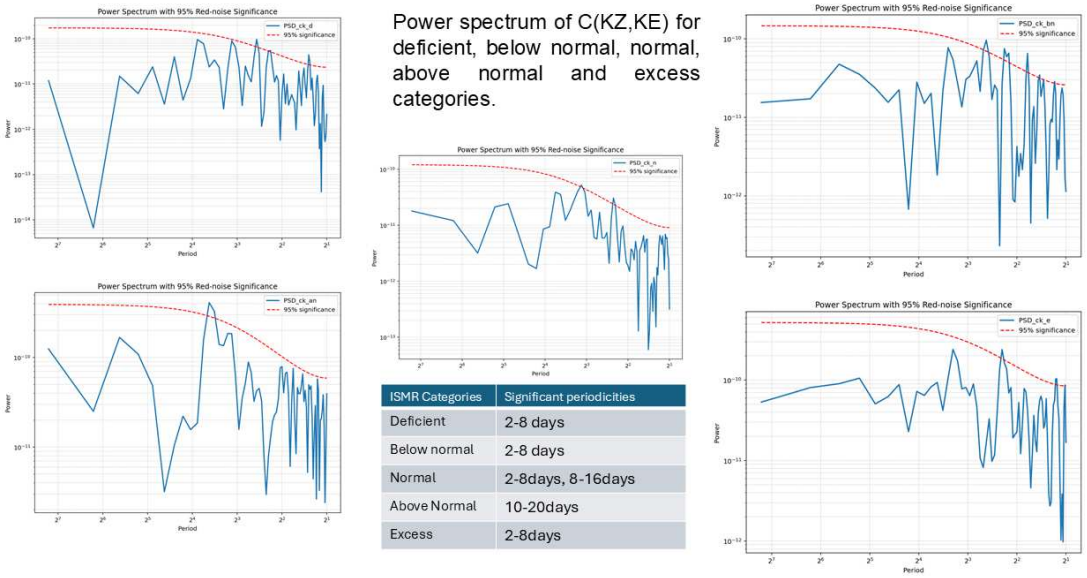
4.6. **Conversion of zonal kinetic energy to eddy kinetic energy [$C(K_Z, K_E)$].**

4.6.1. **Interpretation**: Conversion of ZKE to EKE, denoted by $C(K_Z, K_E)$ is mathematically expressed as,

$$C(K_Z, K_E) = \frac{1}{g}\left\{\begin{array}{c}\int_{100}^{P_s} \frac{\partial[u]}{a\partial\varphi}\overline{u'v'}dp + \int_{100}^{P_s}\overline{\left[v'^2\frac{\partial[v]}{a\partial\varphi}\right]}dp + \int_{100}^{P_s}\overline{[u'^2[v]]}dp \\ + \int_{100}^{P_s}\overline{\left[\omega' u'\frac{\partial[u]}{\partial p}\right]}dp + \int_{100}^{P_s}\overline{\left[\omega' v'\frac{\partial[v]}{\partial p}\right]}dp\end{array}\right\}$$

This term represents the vertically integrated effect of eddy horizontal momentum flux in presence horizontal shear of zonal mean horizontal wind and that of eddy vertical flux of eddy horizontal momentum in presence of vertical shear of zonal mean horizontal wind. Out of all these six terms, the curvature terms, viz., $\frac{1}{g}\int_{100}^{P_s}\overline{\left[\frac{[v]\tan\varphi}{a}u'^2 + \frac{[u]tan\varphi}{a}\overline{u'v'}\right]}dp$ are very small in the region of study. Remaining four terms represents the conversion of ZKE to EKE through interaction of eddies (u', v', ω') with mean horizontal wind ($[u], [v]$), in presence of meridional $\left(\frac{\partial[u]}{a\partial\varphi}, \frac{\partial[v]}{a\partial\varphi}\right)$ and vertical $\left(\frac{\partial[u]}{\partial p}, \frac{\partial[v]}{\partial p}\right)$shear of zonally averaged zonal and meridional wind. During an active monsoon condition, monsoon trough is stronger, i.e., $\frac{\partial[u]}{a\partial\varphi}$ is large and due to genesis and passage of monsoon lows, depressions, etc., there is strong eddy transport $\overline{u'v'}$, making efficient conversion from ZKE to EKE. This term represents barotropic conversion to eddy kinetic energy.

4.6.2. **Power Spectrum analysis**: Power spectrum analysis performed on the time series of daily composite anomalies of this energetics parameter for different ISMR categories are shown in adjoining figure 11(a-e).

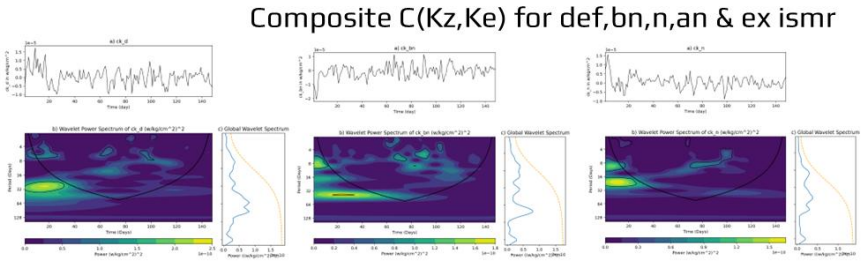


ISMR Categories	Significant periodicities
Deficient	2-8 days
Below normal	2-8 days
Normal	2-8days, 8-16days
Above Normal	10-20days
Excess	2-8days

Fig.11 : PSA of $\boldsymbol{C(K_Z, K_E)}$ for (a) deficient (b)below normal (c) normal (d) above normal (e) excess categories

The figure and the attached table suggest the presence of synoptic scale variation in all ISMR categories, except in above normal category, in which case only QBW mode dominates. This energy conversion is typically associated with barotropic instability, where mean flow feds kinetic energy to the eddies. Thus, the results indicate that in most of the ISMR categories, this barotropic eddy kinetic energy conversion is modulated by high frequency synoptic scale disturbances. The figure suggests that in deficit categories (D & BN), energy transfer is from mean flow to high frequency synoptic scale (2-8 days) disturbances, whereas in the normal and above-normal years it is to both synoptic and quasi-biweekly time scales (8-16 days). From the figure it is seen that in excess ISMR category, barotropic eddy kinetic energy conversion takes place to high frequency synoptic scale disturbances, implying that an enhanced kinetic energy transfer from the zonal flow supports synoptic scale monsoon disturbances to intensify enabling them to produce widespread heavy rainfall.

4.6.3. **Wavelet analysis**: Wavelet analysis performed on the time series of daily composite anomalies of this energetics parameter for different ISMR categories are shown in adjoining figure 12(a-e).



ISMR category	Significant periodicity	Occurrence
Deficient	2-8-day	1-11 & 21-28 Jul, 2-15 Aug
Below-normal	2-8-day	1-17 & 24-30 Jul, 1-6 & 12-16 Aug
Normal	2-8-day	8-11, 16-19 & 27-30 Jul and 1-16 Aug.
Above-Normal	2-8-day 10–20-day	25-29 Jun, 1-7 Jul, 18-24 Jul and 7-21 Aug 11 Jul-2 Aug
Excess	2-8-day 16-32 day	22 Jul-9 Aug & 24-27 Aug 1-8 Jun

Fig.12 : Wavelet analysis of $\boldsymbol{C(K_Z, K_E)}$ for (a) deficient (b)below normal (c) normal (d) above normal (e) excess categories

From the figure and the adjoining table it can be seen that in all five ISMR categories, the time series is dominated by synoptic scale (2-8 days) mode, with time of occurrence differs systematically with monsoon strength, suggesting that even at the synoptic scale, in good monsoon years (Excess, AN) disturbance activity starts earlier and recurs more regularly, while in poor years (Deficient) it is shorter, more sporadic bursts.

The figure show presence of a QBM (10-20 days) mode during 11 Jul–2 Aug in above normal ISMR category suggests a statistically robust quasi-biweekly organization of barotropic KE transfer during peak monsoon. Excess years show an early-season (pre-onset/onset), lower-frequency intraseasonal component during 1–8 June, suggesting that excess years having an organized onset-phase, longer-period (near-monthly) barotropic conversion, possibly tied to the large-scale onset vortex or an early active phase of the 30–60-day intraseasonal oscillation.

5. Summary of the results:

Indian summer Monsoon, primarily driven by convective, radiative and sensible heat sources/sinks; with remarkable features that it occurs every year from June to September and the irregular variation in the amount of seasonal mean rainfall that it brings to India from one year to another and considerable variation within the season, both in space and time, known as Monsoon Intra Seasonal Variation (MISV).

There are lots of studies on Monsoon Intra-seasonal Variability/Oscillation (MISV/MISO), as discussed briefly in the introduction. Generally, for carrying out such studies, primary data such as daily rainfall, OLR, horizontal wind, and cloud pixel data are used.

It is worth noting that ISMR is the final output of various dynamical and thermodynamical processes, such as reverse Hadley circulation, Walker circulation, monsoon-midlatitude flow interaction, diabatic heating, convective instability, etc. Thus, it is envisaged that, along with the known ISO of ISMR, the variability of the processes driving the Monsoon circulation and

599 responsible for the outcome, viz., ISMR, will be examined for a more dynamical interpretation
600 of the ISO of ISMR.
601 Accordingly, in this study, an attempt has been made to revisit Monsoon Intra-seasonal
602 variability/oscillation from the perspective of large-scale atmospheric energetics.
603 Dutta et al. (2019) conducted a study to understand the dynamics of contrasting Indian summer
604 monsoon rainfall (ISMR) across different years during 1979–2017 from the perspective of large-
605 scale atmospheric energetics. For that, daily values of eddy and zonal available potential energy
606 (APE), their generation, eddy and zonal kinetic energy (KE), conversions of zonal KE and eddy
607 APE to eddy KE, and conversions of zonal APE to zonal KE and eddy APE were computed over
608 the region bounded by 65°E–95°E and 5°N–35°N during the period 1 May to 30 September for
609 39 years (1979–2017), using daily ECMWF reanalysed atmospheric data at 0.125° × 0.125°
610 resolution (3 components of wind and temperature). From the daily data, using the Jack-Knife
611 technique, daily composite anomaly of each of these large-scale energetics parameters was
612 computed in their study for different ISMR categories, viz., deficient, below normal, normal,
613 above normal & excess ISMR; following the criteria laid down by the India Meteorological
614 Department. Results of their study suggest a stronger-than-normal thermally direct circulation in
615 the zonal-vertical (x-p) plane & a weaker-than-normal thermally direct circulation in the
616 meridional-vertical (y-p) plane in the above-normal & excess ISMR category.
617 In the present study, we have used here daily computed values of composite anomaly of the
618 above-mentioned six large scale atmospheric energetics parameters, viz., Generations of Zonal
619 Available Potential Energy & Eddy Available Potential Energy, Conversions of Zonal Available
620 Potential Energy to Zonal Kinetic Energy, Eddy Available Potential Energy to Eddy Kinetic
621 Energy, Zonal Available Potential Energy to Eddy Available Potential Energy and Zonal Kinetic
622 Energy to Eddy Kinetic Energy, during 1 May -30 September for the period from 1979 to 2017
623 (ECMWF reanalysed atmospheric data at 0.125° × 0.125° resolution not available afterwards).
624 Generation of ZAPE is due to vertically integrated diabatic heating/cooling over warmer/colder
625 latitudinal belts, which occurs during summer in the northern hemisphere, especially over India
626 and neighbouring oceanic regions. Thus, a generation of ZAPE acts as an energy reservoir to
627 drive the forthcoming gigantic southwest monsoon circulation.
628 This study reveals that, across all ISMR categories, ZAPE generation is primarily a high-
629 frequency process throughout the Indian summer monsoon season, emphasizing the dominant
630 role of monsoon depressions, low-pressure systems, and other synoptic disturbances in
631 modulating the meridional covariance between diabatic heating and temperature gradients.
632 Localized 16–32-day oscillation in above-normal monsoon years suggests occasional quasi-
633 biweekly organization of the heating field. Importantly, the absence of a statistically significant
634 20–40-day mode indicates that the generation of ZAPE may not be directly controlled by the
635 canonical monsoon intraseasonal oscillation (MISO).
636 Conversion of ZAPE to ZKE, expressed mathematically as vertically integrated covariance of
637 zonal eddy temperature and vertical velocity. Physically, this term signifies the strength of the
638 mean monsoon circulation, a thermally direct circulation during the ISM in the y-p plane,
639 converting ZAPE to ZKE due to the rising motion of warmer air and the sinking motion of colder
640 air. A more positive value indicates a stronger mean monsoon circulation. Accordingly, it may
641 be thought of serving as a metric of the strength of the mean monsoon circulation during the
642 southwest monsoon season.
643 The combined power spectrum and wavelet analyses demonstrate that this energy conversion
644 process exhibits dominant variability on synoptic (2–8 days), quasi-biweekly (10–20 days), and
645 intraseasonal (16–32 days) time scales, although the importance of these scales varies with ISMR
646 category. Intermittent oscillations of the QBM & EQBM, confined mainly to July-August, in the
647 deficient ISMR category, suggest episodic strengthening of the zonal circulation, whereas, in the
648 below normal category, only a brief emergence of the QBM event in June suggests weak large-

scale organization. The emergence of both QBM and EQBM during late June to August, in the normal ISMR category, suggests a balanced interaction between synoptic disturbances and monsoon intraseasonal oscillations in modulating this conversion process. Above-normal years are seen to be characterized by a prolonged 10–20-day oscillation during June–July, whereas excess monsoon years exhibit an exceptionally persistent 10–20-day signal extending from mid-June to mid-September, suggesting continuous conversion of zonal available potential energy into zonal kinetic energy, supporting a stronger and more organized large-scale monsoon circulation.

Thus, the intensity of ISMR is closely linked not only to the magnitude of the energy conversion but also to the persistence and organization of its intraseasonal variability, with more active monsoons exhibiting longer lasting and more coherent oscillatory energy exchanges.

Conversion of ZAPE to EAPE represents the strength of the combined effect of two processes, viz., eddy meridional flux of temperature in presence of meridional gradient of temperature and vertical flux of temperature under different static stability conditions.

During Indian Summer Monsoon Season, $\frac{\partial T^*}{a\,\partial \varphi} > 0$. Hence, in the presence of any synoptic-scale weather system (LOW/WML/D/DD) over this region, there is southerly (northerly) cold (warm) air transport to the eastern (western) flank and thus converting ZAPE to EAPE.

In case of a mid-latitude westerly belt, where $\frac{\partial T^*}{a\,\partial \phi} < 0$, the northerly cold air advection ($\overline{v'T'} >), associated$ with southward protruding baroclinic waves embedded in the mid-latitude westerly mean flow, results in the reduction in meridional temperature gradient over ISM region, leading to a reduction in ZAPE at the cost of generation of EAPE, thus leading to conversion of ZAPE to EAPE.

For the second term, when there is a local convective instability over any latitudinal belt in the region of study, then $-\frac{\partial T^*}{\partial z} > \frac{g}{C_p} \Rightarrow \frac{\partial T^*}{\partial p} > \frac{\alpha}{C_p} > 0$. Then rising motion $(\omega < 0)$ of warmer $(T' > 0)$ air associated with the convection results in the conversion of ZAPE to EAPE.

From the PSA and wavelet analyses performed on the time series of daily composite anomalies of these energetic parameters for different ISMR categories, it is revealed that the synoptic-scale (2–8-day) mode is a persistent feature of C (AZ, AE) across all five rainfall categories. A robust intraseasonal / quasi-biweekly (10–20 day) signal is additionally present in the Deficient, Normal and Excess categories, but is absent (or not statistically significant) in the Below Normal and Above Normal categories. This intraseasonal band (10-20 days) is most persistent and energetic in the Excess category and most episodic in the Deficient category, while the Normal category shows the broadest temporal extent of significant activity across the season.

The generation of EAPE is due to vertically integrated diabatic heating/cooling over relatively warmer/colder longitudes. From the mathematical expressions, it is clear that $G(A_E)$ represents the process of integrated combined effect of zonal gradient of diabatic heating and that of temperature. With a given E-W temperature gradient, an enhanced diabatic heating (and/or cooling) over warmer (and/or colder) longitudes results in an enhanced generation of A_E.

From the analysis of the results in the previous section, we have seen that, irrespective of the ISMR categories, G(EAPE) is primarily modulated by the high-frequency synoptic-scale mode (2-8 days). This signifies the roles of monsoon lows, depressions, and other synoptic-scale weather systems in SWM in generating EAPE. The difference in modulation lies in the time and duration of occurrence across the season. In case of excess years, it is frequent, repeated, statistically robust, whereas for deficient years, it is more continuous but comparatively weaker activity; above-normal years get a short early burst that doesn't sustain. Only the below-normal category exhibits brief statistically significant 10–20-day and 16–32-day oscillations during June.

Conversion of EAPE to EKE, expressed mathematically as vertically integrated covariance between eddy temperature and eddy diabatic heating, is positive when there is excess diabatic heating/cooling over warmer/cooler longitudes. Physically, it expresses the strength of a thermally direct circulation (Walker Circulation) in the x-p plane.

From the PSA and wavelet analysis, performed on the time series of daily composite anomaly of this energetics parameters for different ISMR categories, it is revealed that the modulation of the conversion of EAPE to EKE is primarily dominated by high frequency synoptic-scale (2–8 day) mode across all ISMR categories, implying the importance of monsoon lows, depressions and mesoscale convective systems in maintaining eddy kinetic energy. Emergence of a 32-64 days band in above-normal years implies that when rainfall is enhanced, energy conversion is being modulated not just by fast synoptic eddies but also by the slower large-scale ISO. The coexistence of three significant bands, viz., 2–4 days, 4–8 days, and 16–32 days, in the excess ISMR category suggests that excess-rainfall years are characterized by a multi-scale energy conversion process rather than being driven by a single dominant timescale.

Thus, the analysis indicates that high-frequency (2-8 days) disturbances are the primary mechanism for converting EAPE into EKE across all ISMR categories; the persistence and organization of intraseasonal oscillations determine whether this conversion remains episodic (deficient and below-normal years) or sustained (above-normal and excess years). Consequently, in the stronger ISMR category, the modulation of this energy conversion process seems to be associated with more coherent multiscale interactions between synoptic disturbances and intraseasonal monsoon oscillations, leading to prolonged active monsoon conditions and increased seasonal rainfall.

Conversion of ZKE to EKE, also known as barotropic conversion to eddy kinetic energy. In a barotropic instability, the eddy grows by this energy conversion. It represents the vertically integrated effect of eddy horizontal momentum flux in the presence of horizontal shear of zonal mean horizontal wind, and that of eddy vertical flux of eddy horizontal momentum in the presence of vertical shear of zonal mean horizontal wind. Out of all these six terms, in their mathematical expressions, as discussed in the earlier section, the curvature terms are very small in the region of study. The remaining four terms represent the conversion of ZKE to EKE through the interaction of eddies with mean horizontal wind in the presence of meridional and vertical shear of zonally averaged horizontal wind. During an active monsoon condition, monsoon trough is stronger, i.e., $\frac{\partial[u]}{a\partial\varphi}$ is large and due to genesis and passage of monsoon lows, depressions, etc., there is strong eddy transport $\overline{u'v'}$, making efficient conversion from ZKE to EKE.

From the PSA and wavelet analysis, performed on the time series of daily composite anomaly of this energetics parameters for different ISMR categories, it follows that, the conversion of zonal kinetic energy to eddy kinetic energy is predominantly governed by synoptic-scale (2–8-day) variability across all ISMR categories, emphasizing the central role of monsoon depressions, low-pressure systems, and other transient disturbances in transferring energy from the large-scale zonal flow to eddies. However, the nature of this conversion varies with monsoon strength. Above-normal ISMR uniquely exhibits a statistically significant 10–20-day quasi-biweekly oscillation, indicating stronger scale interaction between synoptic and intraseasonal monsoon variability. Excess ISMR shows an additional 16–32-day oscillation during the onset phase, suggesting that low-frequency intraseasonal processes initially modulate eddy development before synoptic disturbances become dominant later in the season. In contrast, deficient and below-normal monsoons lack significant intraseasonal periodicities, implying weaker large-scale organization and more episodic eddy generation. Overall, these results indicate that while synoptic disturbances provide the primary mechanism for converting zonal kinetic energy into eddy kinetic energy, stronger monsoon years are characterized by enhanced multiscale interactions that improve the efficiency and persistence of this energy transfer.

6. Conclusions:

- Dominant statistically significant periodicities in $G(A_Z)$occur in the **2–8-day band**, for all ISMR categories, emphasizing the dominant role of synoptic disturbances in modulating the meridional covariance between diabatic heating and temperature gradients. Localized 16–32-day oscillation in above-normal monsoon years suggests occasional quasi-biweekly organization of the heating field.
- For all categories of ISMR, $C(A_Z, K_Z)$, i.e., the strength of mean monsoon circulation, possesses significant oscillation in the synoptic scale (2-8 days), quasi-biweekly (10-20 days) & excess quasi-biweekly (16-32 days) range, with short duration occurrence in June & July for below-normal & deficient ISMR categories and longer period occurrence from mid-June to mid-July and mid-June to mid-September for above normal & excess categories. It also shows oscillation in the MISO range (30-60 days) in the normal ISMR category.
- Synoptic-scale (2–8 day) mode is a persistent feature of $C(A_Z, A_E)$ across all five rainfall categories. A robust intraseasonal / quasi-biweekly (10–20 day) signal is additionally present in the Deficient, Normal and Excess categories, but is absent (or not statistically significant) in the Below Normal and Above Normal categories. This intraseasonal band (10-20 days) is most persistent in the Excess category and most episodic in the Deficient category.
- Irrespective of the ISMR categories, $G(A_E)$is mostly modulated by high frequency synoptic scale mode (2-8 days), signifying the importance of synoptic scale weather systems. In the excess category, it is a frequent, repeated, statistically robust but comparatively weaker activity in the deficient category. Only the below-normal category exhibits brief statistically significant 10–20-day and 16–32-day oscillations during June.
- There is synoptic-scale (2–8 day) variability in $C(A_E, K_E)$i.e., in the strength of Walker circulation, across all ISMR categories, indicating the importance of synoptic scale weather systems in ISM for this baroclinic eddy kinetic energy conversion. Besides, in above-normal and excess monsoon years, the presence of sustained 16–32-day and/or 30–60-day variability helps maintain efficient baroclinic energy conversion over extended periods.
- Daily composite anomaly of $C(K_Z, K_E)$ in all ISMR categories is dominated by synoptic scale (2-8 days) mode, with time of occurrence differing systematically with monsoon strength. Emergence of a QBW (10-20 days) mode during 11 Jul–2 Aug in the above normal ISMR category and a low frequency oscillation (16-32 days) in the excess category suggests a statistically robust quasi-biweekly organization of barotropic KE transfer during peak monsoon and an organized onset-phase, longer-period barotropic EKE conversion.

Acknowledgement: First author wishes to express his sincere thanks to the Director, IITM and Project Director, DESK, IITM, for providing infrastructure support to carry out this study and also useful & valuable discussions with Dr.M.Rajeevan, former Secretary, MoES, Dr. R.H.Kulkarni, former scientist, IITM and Dr. Aswini Kulkarni, former scientist, IITM, are acknowledged with thanks.

Data declaration: Computation made in this study is based on the output daily energetics values computed in Dutta et al., (2019). Daily energetics data were computed using the data downloaded using the link http://data-portal.ecmwf.int/ data/d/interim_full_daily/levtype=pl for the months May - September for the years 1979–2017. These computed daily energetics data will be made available on reasonable request.

Funding Declaration: No funding used for this work.

Competing Interest declaration. There are no Competing Interests

Author Contribution declaration: Conceptualization of the problem addressed, computation, writing the draft manuscript by SD. Manuscript has been checked and

793 improved using valuable inputs provided by PSM and SGN. PP has provided valuable
794 inputs on recent studies.
795
796 **References:**

797 Abhik, S., Mukhopadhyay, P., Krishna, R. P. M., Salunke, K. D., Dhakate, A. R., & co-authors
798 (2015). Diagnosis of boreal summer intraseasonal oscillation in high-resolution NCEP Climate
799 Forecast System. Climate Dynamics. https://doi.org/10.1007/s00382-015-2769-9

800 Annamalai, H., & Slingo, J. M. (2001). Active/break cycles: Diagnosis of the intraseasonal
801 variability of the Asian summer monsoon. Climate Dynamics, 18, 85–102.

802 Dakshinamurthy, J., and R. N. Keshavamurthy, 1976: On oscillations of period around
803 one month in the Indian summer monsoon. *Indian J. Meteor. Geophys.,* **27,** 201–203.

804 Dutta, S., Narkhedkar, S.G., Mukhopadhyay, P. *et al.* Use of large-scale atmospheric
805 energetics for understanding the dynamics of contrasting Indian summer monsoon
806 rainfall in different years. *Meteorol Atmos Phys* **131**, 945–956 (2019).
807 https://doi.org/10.1007/s00703-018-0610-9

808 Gadgil, S., & Asha, G. (1992). Intraseasonal variation of the summer monsoon I: Observational
809 aspects. Journal of the Meteorological Society of Japan, 70, 517–527.

810 Goswami, B. N., D. Sengupta, and G. Suresh Kumar, 1998: Intraseasonal oscillations and
811 interannual variability of surface winds over the Indian monsoon region. *Proc. Indian*
812 *Acad., Sci., Earth Planet. Sci.,* **107,** 45–64.

813 Goswami, B. N., & Ajaya Mohan, R. S. (2001). Intraseasonal oscillations and interannual
814 variability of the Indian summer monsoon. Journal of Climate, 14, 1180–1198.

815 Hartmann, D. L., & Michelsen, M. L. (1989). Intraseasonal periodicities in Indian rainfall.
816 Journal of the Atmospheric Sciences, 46, 2838–2862.

817 Hartmann, D. L., Michelsen, M. L., & Klein, S. A. (1992). Seasonal variations of tropical
818 intraseasonal oscillations: A 20–25-day oscillation in the western Pacific. Journal of the
819 Atmospheric Sciences, 49, 1277–1289.

820 Hayashi, Y. (1982). Space–time spectral analysis and its application to atmospheric waves.
821 Journal of the Meteorological Society of Japan, 60, 156–171.

822 Hendon, H. H., & Salby, M. L. (1994). The life cycle of the Madden–Julian Oscillation. Journal
823 of the Atmospheric Sciences, 51, 2225–2237.

824 Julian, P. R., & Madden, R. A. (1981). Comments on a paper by T. Yasunari: A quasi-stationary
825 appearance of 30- to 40-day period in the cloudiness fluctuations during the summer monsoon
826 over India. Journal of the Meteorological Society of Japan, 59, 435–437.

827 Kalnay, E., et al. (1996). The NCEP/NCAR 40-year reanalysis project. Bulletin of the American
828 Meteorological Society, 77, 437–471.

829 Keshavamurthy, R. N., 1973: Power spectra of large-scale disturbances of the Indian
830 south-west monsoon. *Indian J. Meteor. Geophys.,* **24,** 117–124.

Kiladis, G. N., & Weickmann, K. M. (1992). Circulation anomalies associated with tropical convection during northern winter. Monthly Weather Review, 120, 1900–1923.

Knutson, T. R., & Weickmann, K. M. (1987). 30–60-day atmospheric oscillations: Composite life cycles of convection and circulation anomalies. Monthly Weather Review, 115, 1407–1436.

Knutson, T. R., Weickmann, K. M., & Kutzbach, J. E. (1986). Global-scale intraseasonal oscillations of outgoing longwave radiation and 250-mb zonal wind during Northern Hemisphere summer. Monthly Weather Review, 114, 605–623.

Konda, G., Chowdary, J.S., Gnanaseelan, C. *et al.* Robust Increase in Indian Summer Monsoon Intraseasonal Variability in a Warmer Climate. *Adv. Atmos. Sci.* **43**, 1079–1091 (2026). https://doi.org/10.1007/s00376-025-5031-3

Kottapalli, Aditya. And Vinayachandran, P. N. (2025), Equatorial convection controls boreal summer intraseasonal oscillations in the present and future climates, *npj | climate and atmospheric science,* https://doi.org/10.1038/s41612-025-00959-4.

Krishnamurti, T. N., & Ardanuy, P. (1980). The 10- to 20-day westward propagating mode and "breaks in the monsoons." Tellus, 32, 15–26.

Krishnamurti, T. N., & Bhalme, H. N. (1976). Oscillations of a monsoon system. Part I: Observational aspects. Journal of the Atmospheric Sciences, 33, 1937–1954.

Krishnamurti, T. N., & Subrahmanyam, D. (1982). The 30–50-day mode at 850 mb during MONEX. Journal of the Atmospheric Sciences, 39, 2088–2095.

Krishnamurthy, V., & Shukla, J. (2000). Intraseasonal and interannual variability of rainfall over India. Journal of Climate, 13, 4366–4377.

Krishnan, R., Zhang, C., & Sugi, M. (2000). Dynamics of breaks in the Indian summer monsoon. Journal of the Atmospheric Sciences, 57, 1354–1372.

Lal, M., Singh, K. K., Srinivasan, G., Rathore, L. S., Naidu, D., & Tripathi, C. N. (1999). Growth and yield responses of soybean in Madhya Pradesh, India to climate variability and change. Agricultural and Forest Meteorology, 93, 53–70.

Lau, K.-H., & Lau, N.-C. (1990). Observed structure and propagation characteristics of tropical summertime synoptic-scale disturbances. Monthly Weather Review, 118, 1888–1913.

Lau, K.-M., & Chan, P. H. (1986). Aspects of the 40–50 day oscillation during the northern summer as inferred from outgoing longwave radiation. Monthly Weather Review, 114, 1354–1367.

Lau, K.-M., & Peng, L. (1990). Origin of low-frequency (intraseasonal) oscillations in the tropical atmosphere. Part III: Monsoon dynamics. Journal of the Atmospheric Sciences, 47, 1443–1462.

Lau, W. K. M., & Waliser, D. E. (Eds.). (2012). Intraseasonal Variability in the Atmosphere-Ocean Climate System (2nd ed.). Springer. https://doi.org/10.1007/978-3-642-13914-7

Lawrence, D. M. (1999). Intraseasonal variability of the South Asian monsoon (Doctoral dissertation). Department of Astrophysical, Planetary, and Atmospheric Sciences, University of Colorado.

Lawrence, D. M., & Webster, P. J. (2002). The boreal summer intraseasonal oscillation: Relationship between northward and eastward movement of convection. Journal of the Atmospheric Sciences, 59, 1593–1606.

Liebmann, B., & Smith, C. A. (1996). Description of a complete (interpolated) outgoing longwave radiation dataset. Bulletin of the American Meteorological Society, 77, 1275–1277.

Lin, T.-H., M.-M. Lu and T. Li, 2025: Influence of northward-propagating intraseasonal oscillations and ENSO background states on summer monsoon onset over the Arabian Sea and India. Climate Dynamics, 63. https://doi.org/10.1007/s00382-025-07587-x

Li, Y., et al., 2022: Maintenance of Cyclonic Vortex During Monsoon Intraseasonal Oscillation: A View From Kinetic Energy Budget. Geophysical Research Letters, 49, e2022GL097740. https://doi.org/10.1029/2022GL097740

Lu, T., G. Huang et al., 2025: Energetic processes underlying the interannual variability of South Asian summer monsoon. npj Climate and Atmospheric Science, 8, 300. https://doi.org/10.1038/s41612-025-01143-4

Madden, R. A. (1986). Seasonal variations of the 40–50 day oscillation in the tropics. Journal of the Atmospheric Sciences, 43, 3138–3158.

Madden, R. A., & Julian, P. R. (1971). Detection of a 40–50 day oscillation in the zonal wind in the tropical Pacific. Journal of the Atmospheric Sciences, 28, 702–708.

Madden, R. A., & Julian, P. R. (1972). Description of global-scale circulation cells in the tropics with a 40–50 day period. Journal of the Atmospheric Sciences, 29, 1109–1123.

Madden, R. A., & Julian, P. R. (1994). Observations of the 40–50 day tropical oscillation — A review. Monthly Weather Review, 122, 814–837.

Maloney, E. D., & Hartmann, D. L. (1998). Frictional moisture convergence in a composite life cycle of the Madden–Julian Oscillation. Journal of Climate, 11, 2387–2403.

Matthews, A. J., Hoskins, B. J., Slingo, J. M., & Blackburn, M. (1996). Development of convection along the SPCZ within a Madden–Julian Oscillation. Quarterly Journal of the Royal Meteorological Society, 122, 669–688.

Mehta, V. M., & Krishnamurti, T. N. (1988). Interannual variability of the 30–50-day wave motion. Journal of the Meteorological Society of Japan, 66, 535–548.

Murakami, T. (1976). Cloudiness fluctuations during the summer monsoon. Journal of the Meteorological Society of Japan, 54, 175–181.

Murakami, T., T. Nakazawa and J. He, 1984: On the 40–50-day oscillation during 1979 Northern Hemisphere summer. Part 1: Phase propagation. *J. Meteor. Soc. Japan,* **62,** 440–468.

Pathak, A., Ghosh, S., Kumar, P., et al. (2017). Role of oceanic and terrestrial atmospheric moisture sources in intraseasonal variability of Indian summer monsoon rainfall. Scientific Reports, 7, 12729. https://doi.org/10.1038/s41598-017-13115-7

Raghavan, K., Sikka, D. R., & Gujar, S. V. (1975). The influence of cross-equatorial flow over Kenya on the rainfall of western India. Quarterly Journal of the Royal Meteorological Society, 101, 1003–1004.

Ramamurthy, K. (1969). Monsoons of India: Some aspects of the 'break' in the Indian southwest monsoon during July and August (Forecasting Manual No. IV-18.3). India Meteorological Department, Pune.

Rodwell, M. J. (1997). Breaks in the Asian monsoon: The influence of Southern Hemisphere weather systems. Journal of the Atmospheric Sciences, 54, 2597–2611.

Salby, M. L., & Hendon, H. H. (1994). Intraseasonal behavior of clouds, temperature, and motion in the tropics. Journal of the Atmospheric Sciences, 51, 2207–2224.

Sardeshmukh, P. D., & Hoskins, B. J. (1988). The generation of global rotational flow by steady idealized tropical divergence. Journal of the Atmospheric Sciences, 45, 261–278.

Sikka, D. R., & Gadgil, S. (1980). On the maximum cloud zone and the ITCZ over Indian longitudes during the southwest monsoon. Monthly Weather Review, 108, 1840–1853.

Singh, S. V., & Kripalani, R. H. (1985). The south to north progression of rainfall anomalies across India during the summer monsoon season. Pure and Applied Geophysics, 123, 624–637.

Slingo, J. M., et al. (1996). Intraseasonal oscillations in 15 atmospheric general circulation models: Results from an AMIP diagnostic subproject. Climate Dynamics, 12, 325–357.

Sperber, K. R., & Annamalai, H. (2008). Coupled model simulations of boreal summer intraseasonal (30–50 day) variability, Part I: Systematic errors and caution on use of metrics. Climate Dynamics, 31, 345–372.

Srinivasan, J., Gadgil, S., & Webster, P. J. (1993). Meridional propagation of large-scale monsoon convective zones. Meteorology and Atmospheric Physics, 52, 15–35.

Wang, B., & Rui, H. (1990). Synoptic climatology of transient tropical intraseasonal convection anomalies: 1975–1985. Meteorology and Atmospheric Physics, 44, 43–61.

Wang, B., & Xie, X. (1997). A model for the boreal summer intraseasonal oscillation. Journal of the Atmospheric Sciences, 54, 72–86.

Waje, S., S. Joseph, M. Phani et al., 2025: Role of Quasi-Biennial Oscillation in modulating subseasonal to seasonal variability of Indian Summer Monsoon. Climate Dynamics, 63, 248. https://doi.org/10.1007/s00382-025-07738-0

Webster, P. J. (1972). Response of the tropical atmosphere to local steady forcing. Monthly Weather Review, 100, 518–541.

Webster, P. J. (1983). Mechanisms of low-frequency variability: Surface hydrological effects. Journal of the Atmospheric Sciences, 40, 2110–2124.

941 Webster, P. J., Magaña, V. O., Palmer, T. N., Shukla, J., Tomas, R. A., Yanai, M., & Yasunari,
942 T. (1998). Monsoons: Processes, predictability, and the prospects for prediction. Journal of
943 Geophysical Research, 103, 14451–14510.

944 Weickmann, K. M., Lussky, G. R., & Kutzbach, J. E. (1985). Intraseasonal (30–60 day)
945 fluctuations of outgoing longwave radiation and the 250 mb streamfunction during northern
946 winter. Monthly Weather Review, 113, 941–961.

947 Wheeler, M., & Kiladis, G. N. (1999). Convectively coupled equatorial waves: Analysis of
948 clouds and temperature in the wavenumber–frequency domain. Journal of the Atmospheric
949 Sciences, 56, 374–399.

950 Yasunari, T. (1979). Cloudiness fluctuations associated with the Northern Hemisphere summer
951 monsoon. Journal of the Meteorological Society of Japan, 57, 227–242.

952 Yasunari, T. (1980). A quasi-stationary appearance of 30- to 40-day period in the cloudiness
953 fluctuations during the summer monsoon over India. Journal of the Meteorological Society of
954 Japan, 58, 225–229.

955 Yasunari, T. (1981). Structure of the Indian monsoon system with around 40-day period. Journal
956 of the Meteorological Society of Japan, 59, 225–229.

957 Zhang, C., & Hendon, H. H. (1997). Propagating and standing components of the intraseasonal
958 oscillation in tropical convection. Journal of the Atmospheric Sciences, 54, 741–752.**54 ,** 741–
959 752.

960

Table-1

Year	% OF LPA	AIRF Cat	Year	% OF LPA	AIRF Cat
1979	81	D	1998	104	N
1980	103.9	N	1999	95.6	BN
1981	99.8	N	2000	92.2	BN
1982	85.5	D	2001	92.2	BN
1983	113	E	2002	80.8	D
1984	95.6	BN	2003	102.3	N
1985	92.9	BN	2004	86.2	D
1986	87.3	D	2005	98.7	N
1987	80.6	D	2006	99.6	N
1988	119.3	E	2007	105.7	AN
1989	100.9	N	2008	98.3	N
1990	106.2	AN	2009	78.2	D
1991	90.7	BN	2010	102	N
1992	93.3	BN	2011	101.6	N
1993	99.1	N	2012	92.9	BN
1994	112.5	E	2013	105.6	AN
1995	98.1	N	2014	88.1	D
1996	103.4	N	2015	85.7	D
1997	102.2	N	2016	97.4	N
			2017	95	BN

Table-2

Illustration of symbols

Sr. No	Symbols	Illustration
1	A_E	Eddy available potential energy
2	A_Z	Zonal available potential energy
3	K_E	Eddy kinetic energy
4	K_Z	Zonal kinetic energy
5	$G(A_Z)$	Generation of Zonal available potential energy
6	$G(A_E)$	Generation of eddy available potential energy
7	$C(A_E, K_E)$	Conversion of Eddy available potential energy to Eddy kinetic energy
8	$C(A_Z, K_Z)$	Conversion of zonal available potential energy to zonal kinetic energy
9	$C(K_Z, K_E)$	Conversion of zonal kinetic energy to Eddy kinetic energy
10	$C(A_Z, A_E)$	Conversion of zonal available potential energy to Eddy available potential energy
11	[S]	Zonal average of 'S'=$\frac{1}{\lambda_e-\lambda_w}\int_{\lambda_w}^{\lambda_e} S d\lambda$
12	$\overline{S}$	Area average of 'S' $=\frac{1}{\sin\varphi_n-\sin\varphi_s}\int_{\varphi_s}^{\varphi_n} S\cos\varphi\, d\varphi$
13	S''	Departure from area average of 'S' $= S - \bar{S}$
14	S'	Departure from zonal average of 'S' $= S - [S]$
15	S^*	Departure of zonal average from area average of 'S' $= [S] - \bar{S}$
Mathematical expression of different terms		

	A_Z	$\int_{100}^{P_s} \frac{\overline{T^{*2}}}{2\sigma} dp$
	A_E	$\int_{100}^{P_s} \frac{\overline{T'^2}}{2\sigma} dp$
	K_Z	$\frac{1}{2g}\int_{100}^{P_s} \overline{([u]^2 + [v]^2)} dp,$
	K_E	$\frac{1}{2g}\int_{100}^{P_s} \overline{(u'^2 + v'^2)} dp$
	$G(A_Z)$	$\frac{R_d}{C_p}\oint \frac{[\theta]^*\left[\dot{Q}\right]^*}{p\left(-\frac{\partial\overline{\theta}}{\partial p}\right)} dm$
	$G(A_E)$	$\frac{R_d}{C_p}\oint \frac{\theta'\dot{Q}'}{p\left(-\frac{\partial\overline{\theta}}{\partial p}\right)} dm$
	$C(A_Z, A_E)$	$-\int_{100}^{\mathrm{P_s}} \left[\overline{\frac{1}{\sigma}\mathrm{v'T'}\frac{\partial \mathrm{T^*}}{\mathrm{a}\,\partial\emptyset}} + \overline{\frac{1}{\sigma}\omega'\mathrm{T'}\frac{\partial \mathrm{T^*}}{\partial \mathrm{p}}}\right] \mathrm{dp}$
	$C(K_Z, K_E)$	$\frac{1}{g}$ $\left\{\begin{array}{c} \int_{100}^{P_s}\left[\cos\varphi u'v'\frac{\partial}{a\partial\varphi}\left[\frac{[u]}{\cos\varphi}\right]\right]dp \\ +\int_{100}^{P_s}\overline{\left[v'^2\frac{\partial[v]}{a\partial\varphi}\right]}dp + \int_{100}^{P_s}\overline{\left[\frac{\tan\varphi}{a}u'^2[v]\right]}dp \\ +\int_{100}^{P_s}\overline{\left[\omega'u'\frac{\partial[u]}{\partial p}\right]}dp + \int_{100}^{P_s}\overline{\left[\omega'v'\frac{\partial[v]}{\partial p}\right]}dp \end{array}\right\}$
	$C(A_E, K_E)$	$-\frac{1}{g}\int_{100}^{P_s}\frac{R}{p}\overline{\omega'T'}dp$

	$C(A_Z, K_Z)$	$-\frac{1}{g}\int_{100}^{P_s}\frac{R}{p}\overline{\omega^* T^*}dp$

974